Proceedings of the 21th National and 10th International Conference of Manufacturing Engineering
February 25-27, 2025, Supplying Automotive Parts Company (SAPCO), Tehran, Iran

Application of SBFEM in Investigating the Defected Square Nano-Graphene Sheets

Mehdi Hajian[1*], Mehrdad Honarmand[2], Alireza Hajian[3]

[1*] Faculty Member, Department of Mechanical Engineering, National University of Skills (NUS), Tehran, Iran — Mhajian@nus.ac.ir
[2] Faculty Member, Department of Mechanical Engineering, Tiran Branch, Islamic Azad University, Tiran, Iran — Mehrdad.honarmand@iau.ac.ir
[3] Faculty Member, Department of Physics, Najafabad Branch, Islamic Azad University, Najafabad, Iran — Dralirezahajian@gmail.com

Abstract

In this article, using the scaled boundary finite element semi-analytical method, complete graphene nanosheets with simulated structural defects and its mechanical behavior were investigated. In this analysis, the atomic bond between carbon atoms was modeled with a rod with a circular cross section and then scaled boundary finite element relationships were projected based on the model geometry. The comparison of the results obtained from the scaled boundary finite element method with molecular dynamics showed that this analysis method can be used with high accuracy as a continuous medium method in the mechanical analysis of complete or structurally defective nanographene sheets. The existence of a structural defect significantly reduces the strength and strain of the nanographene sheet in such a way that the stress of breaking is reduced by more than 34% and the strain of breaking is reduced by more than 50%. Also, if instead of the rod element, the nanographene plate is considered a continuous medium plate, and in order to create a geometry identical to the problems with the rod element, the material-free medium is simulated with zero elastic modulus elements. The results will not have the same accuracy as the results with the bar element.

Keywords: Scaled finite boundary element, square nano-graphene sheet, structural defects, mechanical behavior, molecular dynamics

کاربرد روش المان محدود مرزی مقیاس شده در ارزیابی صفحات نانوگرافن مربعی معیوب

مهدی حاجیان[1*]، مهرداد هنرمند[2]، علیرضا حاجیان[3]

[1*] عضو هیات علمی، گروه مهندسی مکانیک، دانشگاه ملی مهارت، تهران، ایران — Mhajian@nus.ac.ir
[2] استادیار گروه مکانیک، دانشکده فنی و مهندسی، واحد تیران، دانشگاه آزاد اسلامی، تیران، ایران — Mehrdad.honarmand@iau.ac.ir
[3] استادیار گروه فیزیک، دانشکده فیزیک، واحد نجف آباد، دانشگاه آزاد اسلامی،نجف آباد، ایران — Dralirezahajian@gmail.com

چکیده

در این مقاله با استفاده از روش نیمه تحلیلی المان محدود مرزی مقیاس شده، نانوصفحات کامل مربعی گرافن با عیوب ساختاری شبیه سازی شده و رفتار مکانیکی آن مورد بررسی قرار گرفت. در این تحلیل، پیوند اتمی بین اتم‌های کربن با یک میله با مقطع دایره‌ای مدل‌سازی شد و سپس روابط اجزای محدود مرزی مقیاس‌بندی شده بر اساس هندسه مدل پیش‌بینی شد. مقایسه نتایج به‌دست‌آمده از روش اجزای محدود مرزی مقیاس‌شده با دینامیک مولکولی نشان داد که این روش آنالیز می‌تواند با دقت بالایی به عنوان یک روش محیط پیوسته در آنالیز مکانیکی ورق‌های نانوگرافن کامل یا معیوب ساختاری استفاده شود. وجود عیب ساختاری استحکام و کرنش ورق نانوگرافن را به میزان قابل توجهی کاهش می دهد به گونه ای که تنش شکست بیش از ۳۴ درصد و کرنش شکست بیش از ۵۰ درصد کاهش می یابد. همچنین اگر به جای عنصر میله، ورق نانوگرافن یک صفحه متوسط پیوسته در نظر گرفته شود و به منظور ایجاد هندسه ای مشابه با مشکلات عنصر میله، محیط بدون مواد با عناصر مدول الاستیک صفر شبیه سازی شود. نتایج به اندازه نتایج با عنصر نوار دقتی ندارند.

کلیدواژه‌ها: المان مرزی محدود مقیاس شده، نانوصفحات مربعی گرافن، عیوب ساختاری، رفتار مکانیکی، دینامیک مولکولی.

Introduction

Graphene, as a two-dimensional material, with remarkable electrical, thermal and mechanical properties, has attracted the attention of many researchers in the last few decades. This material with elastic modulus and strength of 1TPa and 130GPa, respectively, is considered one of the best options for strengthening nanocomposites and electronic devices in micro-nano dimensions [1].

Many efforts have been made to determine the mechanical properties and to model the behavior of graphene nanosheets.

Emelchenko et al. (1997) investigated the fracture dynamics of nano-graphene plates of the chair handle and obtained the value of the stress intensity factor using Griffith's energy theory (4.7-6 Mpa√m)[2].

Zhang et al. (2012) investigated the fracture and crack growth in a graphene nanosheet under shear stress loading and the second crack mode using molecular dynamics. They proved that the crack growth depends on the phase angle, which is a multiple of 30 degrees compared to the crack opening line [3].

Khar et al. (2007) investigated the mechanical properties of graphene nanosheets with large cracks by simultaneously using continuum mechanics and molecular dynamics. They found that the cross-sectional area of defects, perpendicular to the loading direction, has a greater effect than the same The size of cracks and defects is in other directions. They also proved that in flawed plates with a size of 10 Angstroms, the fracture stress calculation with the used method is very consistent with Griffith's relations [4].

Zhou et al. (2012) calculated the value of the stress intensity factor for the chair arm 4.21Mpa√m and for the zigzag 3.71Mpa√m. They also showed that in the zigzag nanoplates the crack growth is regular and similar, but in the armchair plates it is irregular. is[5].

Devapriya et al. (2014) obtained the fracture of graphene nanosheets using molecular dynamics and calculating integral J at different temperatures and showed that the critical value of J depends on the crack length [6].

Min Cui et al. (2014) investigated the fracture and crack growth in a chair handle nanographene plate under prestress using molecular dynamics. In this article, they proved that for atomic bond fracture in carbon, the bond length must be stretched to 100%. [7].

Hanking-Yen et al. (2015) used the Griffith criterion for the growth of the nanographene plate and proved that the Griffith criterion can also be used for the nanographene structure in sizes less than 10 nanometers, but it calculates the fracture stress to a lesser extent. [8].

J. Li Tsai et al. (2009) investigated the fracture and crack growth by the method of continuous environment mechanics and molecular dynamics and proved that the strain energy released in both methods is equal with a small difference and suggested that the strain energy released can be be used as a parameter in modeling the failure of nanographene sheets [9].

The scaled boundary finite element method is a new semi-analytical method that is used to solve equations with partial derivatives. In this method, which combines the advantages of the finite element and boundary element methods, the discretization is done only on the boundaries, and therefore, like the boundary element method, the dimensions of the problem are reduced to one dimension, and like the finite element method, no fundamental solution is needed. does not have.

Wolf et al. (1995) mentioned relationships based on similarity principles as an alternative to the boundary component method [10].

Song [11], Lindman [12] and Chidgezi [13], using the scaled boundary finite element, investigated the crack growth in different materials and showed that this method as an efficient and high accuracy method can be used in problems benefit failure

From the techniques that have been used so far to study the fracture of nanographene, numerical techniques with high computational cost, such as molecular dynamics or Monte Carlo, can be mentioned, which have various limitations. Many attempts have been made to fill the gap between molecular methods and continuum mechanics, however, a comprehensive method in continuum mechanics to study graphene nanosheets has not yet been found.

In this article, for the first time, the mechanical behavior of nano-graphene has been studied using the scaled boundary finite element method, which, due to the high speed and accuracy of this method, can be a suitable substitute for the finite element in the future.

Scaled boundary finite element relations

In the scaled boundary element, the scale point O is located inside the environment and at a location from which the entire external boundary is visible. By scaling the boundary S in the radial direction relative to the scale point O, using the radial coordinate ξ that is between zero and one, the entire analyzed domain is divided into triangular sections, each of which corresponds to boundary elements Se (Figure 1).

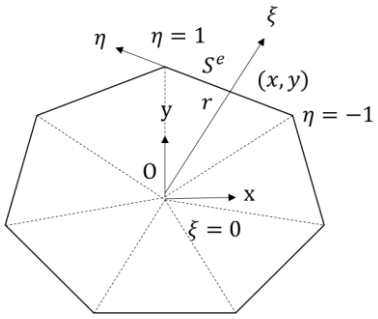

Figure 1: Two-dimensional SBFM coordinates

$$x(\eta) = [N(\eta)]\{x\} \qquad y(\eta) = [N(\eta)]\{y\} \quad (1)$$

In relation (1), η∈[-1,1] is the peripheral coordinate and (y x ,) is the coordinate of the Cartesian points of the beginning and end points of the Se element, i.e. where ξ=1 (relation 2).

$$x = \begin{Bmatrix} x_1 \\ x_2 \end{Bmatrix} \qquad y = \begin{Bmatrix} y_1 \\ y_2 \end{Bmatrix} \quad (2)$$

To obtain the points inside the element, where ξ∈[0,1], relations 3 and 4 are used:

$$x(\xi,\eta) = \xi x(\eta) = \xi[N(\eta)]\{x\} \quad (3)$$

$$y(\xi,\eta) = \xi y(\eta) = \xi[N(\eta)]\{y\} \quad (4)$$

The relationship between the gradient operator in Cartesian coordinates and the scaled boundary element is as follows:

$$\begin{Bmatrix} \frac{\delta}{\delta\xi} \\ \frac{\partial}{\partial\eta} \end{Bmatrix} = [\hat{J}(\xi,\eta)] \begin{Bmatrix} \frac{\delta}{\delta x} \\ \frac{\partial}{\partial\eta} \end{Bmatrix} \quad (5)$$

that the Jacobian matrix is calculated as follows:

$$[\hat{J}(\xi,\eta)] = \begin{bmatrix} 1 & 0 \\ 0 & \xi \end{bmatrix} \begin{bmatrix} x(\eta) & y(\eta) \\ x(\eta)_{,\eta} & y(\eta)_{,\eta} \end{bmatrix} \begin{bmatrix} 1 & 0 \\ 0 & \xi \end{bmatrix} [J(\eta)] \quad (6)$$

The displacement at any point in the polygonal environment is obtained from the following equation:

$$u(\xi,\eta) = N(\eta)u(\xi) \quad (7)$$

In the above relationship, u(ξ) is the displacement at the corner points.
To calculate strains, it is calculated from equation 8:

$$\epsilon(\xi,\eta) = Lu(\xi,\eta) \quad (8)$$

where L is the differential matrix operator:

$$L = b_1(\eta)\frac{\partial}{\partial\xi} + \xi^{-1}b_2(\eta)\frac{\partial}{\partial\eta} \quad (9)$$

In the above equation, the coefficients b_1 and b_2 are:

$$b_1 = \frac{1}{|J(\eta)|}\begin{bmatrix} y(\eta)_{,\eta} & 0 \\ 0 & -x(\eta)_{,\eta} \\ x(\eta)_{,\eta} & y(\eta)_{,\eta} \end{bmatrix} \quad (10)$$

$$b_2 = \frac{1}{|J(\eta)|}\begin{bmatrix} -y(\eta) & 0 \\ 0 & x(\eta) \\ x(\eta) & -y(\eta) \end{bmatrix} \quad (11)$$

The strain at any point of the environment is obtained as follows:

$$\epsilon(\xi,\eta) = B_1(\eta)u(\xi)_{,\xi} + \xi^{-1}B_2(\eta)u(\xi) \quad (12)$$

that B_1 and B_2 are calculated from the following equation:

$$B_1 = b_1(\eta)N(\eta) \quad (13)$$

$$B_2 = b_2(\eta)N(\eta)_{,\eta} \quad (14)$$

The following equation can be used to calculate the stress at any point:

$$\sigma(\xi,\eta) = DB_1(\eta)u(\xi)_{,\xi} + \xi^{-1}DB_2(\eta)u(\xi) \quad (15)$$

By applying the virtual work method to equation 5, the scaled boundary finite element equation that can be solved analytically in the ξ direction is calculated as follows:

$$E_0\xi^2u(\xi)_{,\xi\xi} + (E_0 - E_1 + E_1^T)\xi u(\xi)_{,\xi} - (E_1^T - E_2)u(\xi) = 0 \quad (16)$$

The values of E_0, E_1 and E_2 can be calculated from relations 17, 18 and 19:

$$E_0 = \int_{-1}^{1} B_1(\eta)^T D B_1(\eta)|J(\eta)|d\eta \quad (17)$$

$$E_1 = \int_{-1}^{1} B_2(\eta)^T D B_1(\eta)|J(\eta)|d\eta \quad (18)$$

$$E_2 = \int_{-1}^{1} B_2(\eta)^T D B_2(\eta)|J(\eta)|d\eta \quad (19)$$

Equation 20 can be used to calculate the force at any point:

$$q(\xi) = E_0\xi u(\xi)_{,\xi} + E_1^T u(\xi) \quad (20)$$

To solve the scaled boundary finite element equation (Equation 16), by introducing a variable change, the equation becomes a first-order ordinary differential equation with twice the number of unknowns[14] where the matrix z is the Hamiltonian matrix and the coefficient of the first-order ordinary differential equation is It will be as follows:

$$z = \begin{bmatrix} E_0^{-1}E_1^T & -E_0^{-1} \\ -E_2 + E_1E_0^{-1}E_1^T & -E_0^{-1}E_0^{-1} \end{bmatrix} \quad (21)$$

Equation 22 can be used to calculate eigenvalues and eigenvectors:

$$[z][\phi] = -[\phi][\Lambda] \quad (22)$$

And the eigenvector matrix is as follows:

$$[\phi] = \begin{bmatrix} \phi_{11} & \phi_{12} \\ \phi_{21} & \phi_{22} \end{bmatrix} \quad (23)$$

The hardness matrix can be calculated from equation 24:

$$K = [\phi_{21}][\phi_{11}]^{-1} \quad (24)$$

We will rewrite the relation 7 and 20 respectively:

If the object under analysis is enclosed between two regions ξ=ξ_1 of the inner region and ξ=ξ_2 of the outer region as shown in Figure 2, the integration constants and the stiffness matrix will be calculated as follows:

$$u(\xi) = \phi_{11}\xi^{-\lambda_i}\{c_1\} + \phi_{12}\xi^{-\lambda_i}\{c_2\} \quad (25)$$
$$q(\xi) = \phi_{21}\xi^{-\lambda_i}\{c_1\} + \phi_{22}\xi^{-\lambda_i}\{c_2\} \quad (26)$$

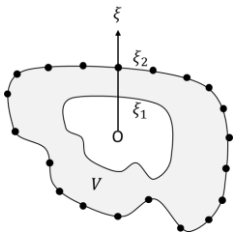

Figure 2: Bounded environment with similar internal and external boundaries

$$\begin{Bmatrix} c_1 \\ c_2 \end{Bmatrix} = \begin{bmatrix} \phi_{11}{\xi_1}^{-\lambda} & \phi_{12}{\xi_1}^{\lambda} \\ \phi_{21}{\xi_2}^{-\lambda} & \phi_{22}{\xi_1}^{\lambda} \end{bmatrix}^{-1} \begin{Bmatrix} u(\xi_1) \\ u(\xi_2) \end{Bmatrix} \quad (27)$$

Modeling of the square nanographene sheet in SBFEM

From the perspective of molecular mechanics dynamics, a graphene nanosheet can be considered as a large molecule containing carbon atoms. Atomic nuclei can be points in matter. Their movement is in the form of a force field that is created by nucleus-electron and nucleus-nucleus interactions. Total potential energy, ignoring electromagnetic interactions, is the sum of energies related to covalence and valence or bonding and non-bonding interactions:

$$U = U_r + U_\theta + U_\phi + U_\omega + U_{vd\omega} \quad (29)$$

where Ur is the interaction effect in bond tension, UΘ is for the angular bending of the bond, Uφ is the effect of bending outside the bond and between two surfaces, Uω is the out-of-surface torsion energy and Uvdω is the energy of non-bond van der Waals interactions, which is shown in Figure 3 .

Assuming that covalent forces between carbon atoms can be replaced by using harmonic functions, the potential energy related to covalent bonds between carbon atoms are defined by the following equations.

$$U_r = \frac{1}{2}k_r(r - r_0)^2 = \frac{1}{2}k_r(\Delta r)^2 \quad (30)$$
$$\boldsymbol{U_\theta = \frac{1}{2}k_\theta(\theta - \theta_0)^2} = \frac{1}{2}k_\theta(\Delta\theta)^2 \quad (31)$$
$$U_\varphi = \frac{1}{2}k_\varphi(\Delta\varphi)^2 \quad (32)$$

which respectively U_r is the tensile energy, U_θ is the bending energy, U_φ is the torsional energy of the bond and k_r, k_θ and k_φ are respectively the coefficients of tension, bending and torsion of the chemical bond, whose values are shown in Table 1 [15]

Table 1: The molecular mechanics constants

coefficient	value
Kθ	8.76 × 10-10 N nm/rad2
Kφ	78 × 10-10 N nm/rad2
Kr	6.52 × 10-7 N/nm

Also, in the above relationships, r_0 θ_0 depends on the distance between atoms and the bond angle in the free state, and the values of r and θ depend on the distance and the bond angle after shape change. As a result, the parameters Δθ, Δr and Δφ indicate the changes in bond length, bond angle and bond twist angle, respectively. In the finite element modeling of the carbon-carbon bond, it is replaced by an isotropic rod element with length L, cross-sectional area A, and moment of inertia I. The strain energy of the beam element with these characteristics under pure axial load N, under bending moment M and under pure torsional moment T are defined as follows:

$$U_N = \int_0^L \frac{N^2}{2EA}dL = \frac{EA}{2L}(\Delta L)^2 \quad (33)$$

$$\boldsymbol{U_M = \int_0^L \frac{M^2}{2EI}dL = \frac{EI}{2L}(2\alpha)^2} \quad (34)$$

$$U_T = \int_0^L \frac{T^2}{2GJ}dL = \frac{GJ}{2L}(2\beta)^2 \quad (35)$$

If in the scaled boundary finite element, the cross section is considered as a circle with radius r, then the radius of the circle will be 0.0733 nm and the elastic modulus will be 5.487 TPa.

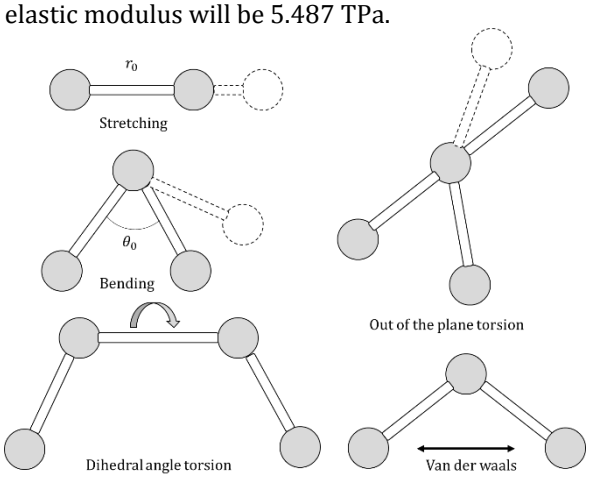

Figure 3: Interatomic interactions in molecular mechanics

Simulating the nanographene sheet in the scaled boundary finite element

To simulate the nanographene sheets, as mentioned before, the atomic bond was converted into a rod with an equivalent cross-sectional area. In this article, all the calculations were done by MATLAB software.

To perform calculations in the scaled boundary finite element, as seen in the figure, each bar is like a continuous medium, which is limited in the coordinates of the scaled boundary element between two coordinates ξ_1≪ξ≪1, the value of ξ_1 according to the calculations Previously and according to Figure 4, it is calculated as follows and it should be noted that L is equal to the initial bond length, 0.142 nm in the center of the connection of each rod and d is the diameter of the rod 0.146 nm:

$$\cos(30) = \frac{d}{x} \xrightarrow{yields} x = \frac{d}{\cos(30)} = 0.168\ nm \quad (36)$$

$$L_0 = L - \frac{x}{2} = 0.142 - 0.084 = 0.058nm \quad (37)$$

$$L_1 = L + \frac{x}{2} = 0.142 + 0.084 = 0.226\text{nm} \quad (38)$$

$$\xi_1 = \frac{L_0}{L_1} = \frac{0.058}{0.226} = 0.256 \quad (39)$$

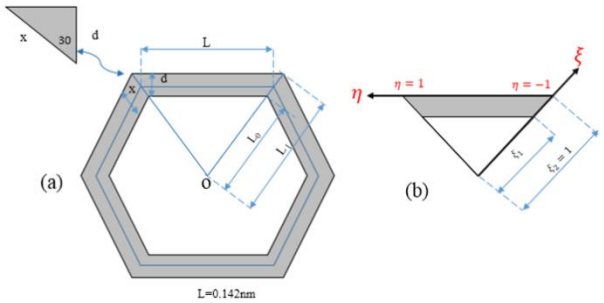

Figure 4: Interatomic interactions in molecular mechanics (a) How to connect the rod elements and (b) the bar element is displayed with scaled boundary finite element coordinates.

The steps of analysis and programming in MATLAB software are as follows:

1- Entry of basic information including network dimensions, elastic modulus, forces, boundary conditions, etc.

2- Using relations 17 to 23, to calculate E_0, E_1, E_2, vector and eigenvalues assuming that the nanographene sheet is a complete element. (Figure 5(a))

3- Calculation of the stiffness matrix of each element from equation 28 for the bar element in the range of 0.256≪ξ≪1. (Figure 5(b))

4- Assembling the hardness matrices of each bar and creating the total hardness matrix k_total

5- Applying point forces and boundary conditions in the relation f=k_total u, calculating the displacements on the perimeter points 1 to 10 for each rod

6- Calculation of integration coefficients using equation 27 for each bar

7- Calculation of stress and strain for each rod using relations 25 and 26

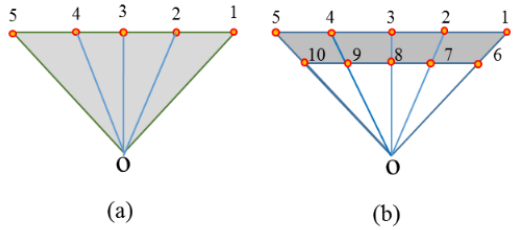

Figure 5: Interatomic interactions in molecular mechanics

Results and Discussion

The examined sample for validation is a defect-free nanographene sheet with dimensions of 25 x 25 angstroms (Figure 6).

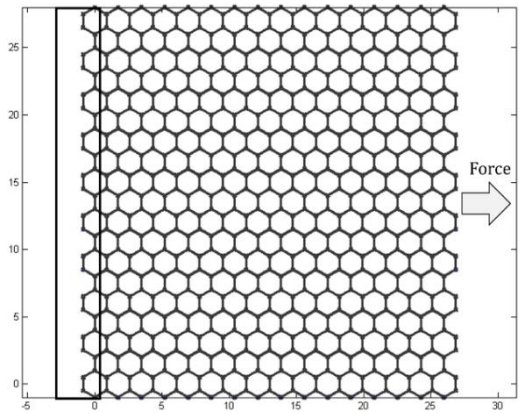

Figure 6: The uniaxial tensile load on a prefect Nano graphene sheet

Figure 7 shows the comparison between stress and strain of nanographene network between two methods of molecular dynamics and scaled boundary finite element.

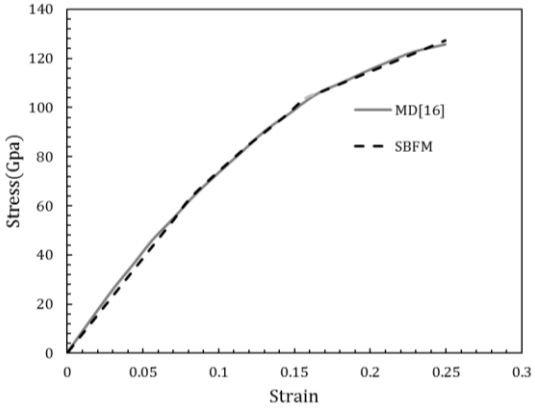

Figure 7: Comparing stress-strain curves of the prefect sample obtained by SBFM and MD

Malkuti et al. (2016) [16] reported the amount of ultimate stress and failure strain through molecular dynamics and by programming in LAMMPS software as 130.92 and 24.8% GPa, respectively, and these values were scaled using boundary finite element, respectively. 127.3 GPa and 24.9% were calculated and with experimental tests, respectively, 130 GPa ± 10 GPa and 25% were reported [17]. As seen in Figure 7, the error rate between the final stress values obtained from molecular dynamics and the scaled boundary finite element is 2.8%. In the scaled boundary element method, according to the equation of the stress-strain relationship with a three-line curve, the graphs obtained are segment by segment straight lines, which increase the amount of stress and as a result of breaking the interatomic bond, the hardness matrix decreases. found and therefore the slope of the stress and strain diagram lines also decreases. But despite this simplification, the accuracy of the obtained results is very significant. With the increase of stress from 100GPa, which is equivalent to 15% strain, the slope of the graph decreases significantly and tends to the asymptotic state to some extent.

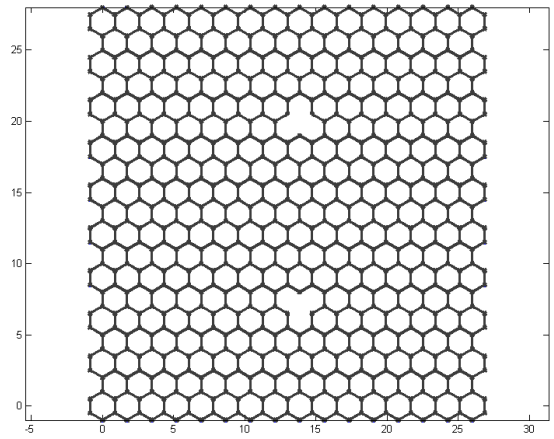

Figure 8: Two vacancies in the line perpendicular to the line load direction

Simulation of nanographene sheet with structural defects

Figures 8 and 9 show a nanographene sheet with a structural defect of the vacancy network. In Figure 8, the network defect includes the absence of 2 carbon atoms and as a result the absence of 6 atomic bonds, and in Figure 9, the network defect includes three carbon atoms, which causes the absence of 9 atomic bonds. In both cases, the vacancy defect is perpendicular to the force line.

As can be seen in Figures 10 and 11, the results are almost in good agreement. By observing and comparing the results of a complete plate with plates with structural defects, it can be seen that the fracture stress values are significantly reduced, so that the fracture stress has decreased from 128 GPa to 77 GPa, so it can be concluded that there is a vacancy defect. It can reduce the strength of a nanographene sheet by about 40%. Another noteworthy point is that the stress-strain relationship in these plates remains almost linear to a large extent. The failure strain is reduced to less than half compared to plates without structural defects.

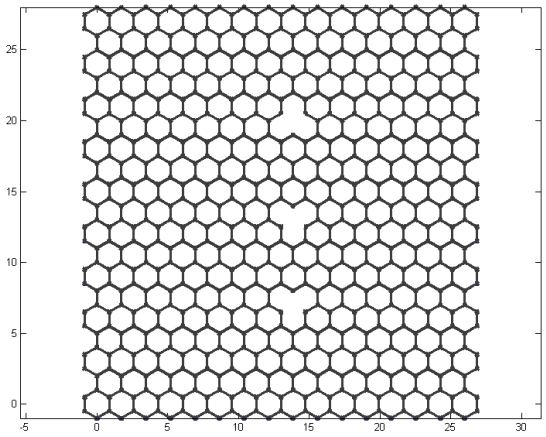

Figure 9: Three vacancies in the line perpendicular to the line load direction

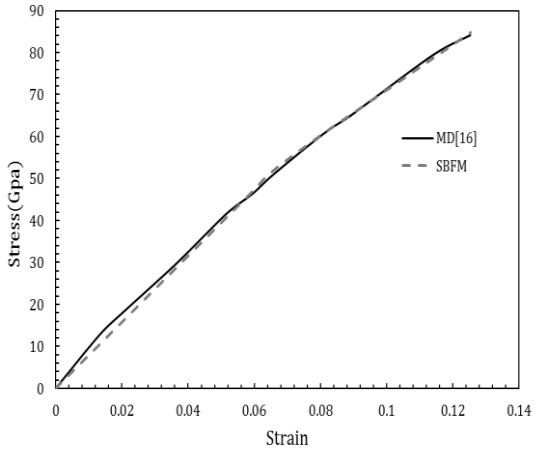

Figure 10: Comparing stress-strain curves of a sample with two vacancies obtained by SBFM and MD

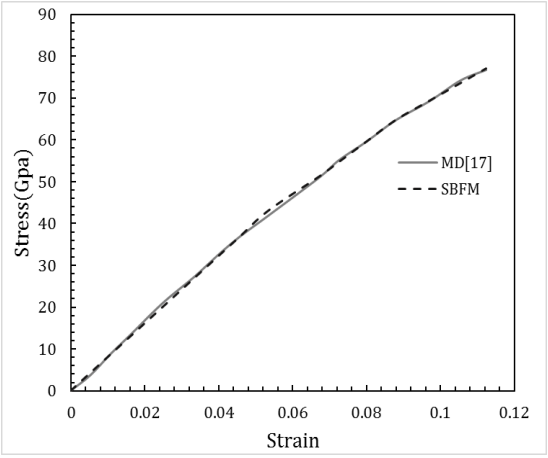

Figure 11: Comparing stress-strain curves of a sample with three vacancies obtained by SBFM and MD

Simulation of nanographene plate with scaled boundary finite element

If in the simulation of graphene nanosheets with a scaled boundary finite element, instead of using a rod element in the simulation, the environment is considered continuous, and in order to create the same geometry as problems with a rod element, the area free of matter with If the elastic coefficient is considered zero, the results will have a significant error.

In Figure 12, the stress-strain diagram for the sample with three blanks is compared in all three methods. As can be seen, in the simulation with the scaled boundary element method with continuous environment, the amount of fracture stress and failure strain will be 79.8 GPa and 11%, respectively, which compared to the scaled boundary element method with rod element and molecular dynamics has an error of 6 % is.

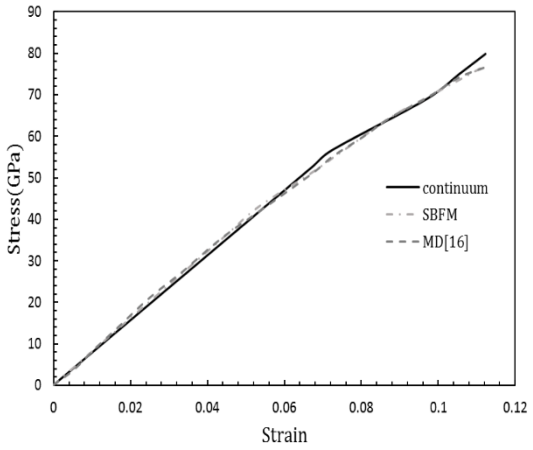

Figur 12: Comparing stress-strain curves of a sample with three vacancies obtained by SBFM with bar element, Continuum and MD

References

[1] F. Meng, C. Chen, J. Song, Lattice trapping and crack decohesion in graphene, Carbon, Vol. 116, pp. 33-39, 2017.

[2] A. Omeltchenko, J. Yu, R. K. Kalia, P. Vashishta, Crack front propagation and fracture in a graphite sheet: a molecular-dynamics study on parallel computers, Physical review letters, Vol. 78, No. 11, pp. 2148, 1997.

[3] B. Zhang, L. Mei, H. Xiao, Nanofracture in graphene under complex mechanical stresses, Applied Physics Letters, Vol. 101, No. 12, pp. 121915, 2012.

[4] R. Khare, S. L. Mielke, J. T. Paci, S. Zhang, R. Ballarini, G. C. Schatz, T. Belytschko, Coupled quantum mechanical/molecular mechanical modeling of the fracture of defective carbon nanotubes and graphene sheets, Physical Review B, Vol. 75, No. 7, pp. 075412, 2007.

[5] Z. Xu, Graphene nano-ribbons under tension, Journal of Computational and Theoretical Nanoscience, Vol. 6, No. 3, pp. 625-628, 2009.

[6] M. Dewapriya, R. Rajapakse, A. Phani, Atomistic and continuum modelling of temperature-dependent fracture of graphene, International Journal of Fracture, Vol. 187, No. 2, pp. 199-212, 2014.

[7] M.-Q. Le, R. C. Batra, Crack propagation in pre-strained single layer graphene sheets, Computational Materials Science, Vol. 84, pp. 238-243, 2014.

[8] Honarmand M, Moradi M. Investigation of mechanical behavior of perfect nano-garphene sheets and defected ones by Scaled boundary finite element method. Modares Mechanical Engineering. 2018 Nov 10;18(7):233-9.

[9] J.-L. Tsai, S.-H. Tzeng, Y.-J. Tzou, Characterizing the fracture parameters of a graphene sheet using atomistic simulation and continuum mechanics, International Journal of Solids and Structures, Vol. 47, No. 3, pp. 503-509, 2010.

[10] J. P. Wolf, C. Song, Dynamic-stiffness matrix in time domain of unbounded medium by infinitesimal finite element cell method, Earthquake Engineering & Structural Dynamics, Vol. 23, No. 11, pp. 1181-1198, 1994.

[11] C. Song, Evaluation of power-logarithmic singularities, T-stresses and higher order terms of in-plane singular stress fields at cracks and multi-material corners, Engineering Fracture Mechanics, Vol. 72, No. 10, pp. 1498-1530, 2005.

[12] J. Lindemann, W. Becker, Analysis of the free-edge effect in composite laminates by the boundary finite element method, Mechanics of composite materials, Vol. 36, No. 3, pp. 207-214, 2000.

[13] S. R. Chidgzey, A. J. Deeks, Determination of coefficients of crack tip asymptotic fields using the scaled boundary finite element method, Engineering Fracture Mechanics, Vol. 72, No. 13, pp. 2019-2036, 2005.

[14] C. Song, A matrix function solution for the scaled boundary finite-element equation in statics, Computer Methods in Applied Mechanics and Engineering, Vol. 193, No. 23, pp. 2325-2356, 2004.

[15] Hajian M, Moradi M. Stochastic fracture analysis of cracked nano-graphene sheets by scaled boundary finite element method. Engineering Analysis with Boundary Elements. 2019 Jan 1;98:54-63..

[16] M. Malakouti, A. Montazeri, Nanomechanics analysis of perfect and defected graphene sheets via a novel atomic-scale finite element method, Superlattices and Microstructures, Vol. 94, pp. 1-12, 2016.

[17] C. Lee, X. Wei, J. W. Kysar, J. Hone, Measurement of the elastic properties and intrinsic strength of monolayer graphene, science, Vol. 321, No. 5887, pp. 385-388, 2008.